A growing structure near the deformation front in SW Taiwan as deduced from SAR interferometry and geodetic observation

Mong-Han Huang,[1] Jyr-Ching Hu,[1] Chia-Sheng Hsieh,[2] Kuo-En Ching,[3] Ruey-Juin Rau,[3] Erwan Pathier,[4] Bénédicte Fruneau,[5] and Benoît Deffontaines[5]

Received 25 December 2005; revised 7 May 2006; accepted 24 May 2006; published 30 June 2006.

[1] We apply the D-InSAR technique to monitor the active growing structure on the Tainan Tableland near the deformation front in SW Taiwan using ERS SAR images in the period of 1996–2000. Interferometric processing of six SAR images reveals the average slant range displacement (SRD) to be ~12.5 mm/yr, and it increases from the west edge of the Tainan Tableland and decreases across the Houchiali fault. The GPS campaign data indicate an average horizontal movement of 12 ± 4 mm/yr in the direction of N44°W for the Tainan Tableland with respect to the western coastline. Five precise leveling surveys across the Tainan Tableland over two years show an uplift rate of ~14 mm/yr for the benchmarks on the Tableland. By combining the horizontal velocity of GPS data and the SRD of D-InSAR we transfer the SRD into vertical deformation and discuss the deformation pattern and seismic hazards in the Tainan area. **Citation:** Huang, M.-H., J.-C. Hu, C.-S. Hsieh, K.-E. Ching, R.-J. Rau, E. Pathier, B. Fruneau, and B. Deffontaines (2006), A growing structure near the deformation front in SW Taiwan as deduced from SAR interferometry and geodetic observation, *Geophys. Res. Lett.*, *33*, L12305, doi:10.1029/2005GL025613.

1. Introduction

[2] Taiwan is one of the most active seismic regions in the world. Historical records indicate more than 12 large (Mw > 6) earthquakes since 1900, including the 1999 Mw 7.6 Chi-Chi earthquake (Figure 1) which occurred in Taiwan and resulted in serious damage and causalities in densely populated areas. The newly initiated blind fault system in the coastal plain area is due to the on-going arc-continent collision and increases potential earthquake hazards in the western alluvial plain where it was once considered less of a threat in comparison with other regions of the island. Tainan Tableland is a significant morphological feature of an active growing structure near the deformation front located in SW Taiwan (Figure 2a). The Tainan City (the fourth largest) with more than 700,000 people is situated on the active structure. Recent research suggests that the Houchiali fault, which located in the east portion of the Tainan Tableland, was an active fault [*Lin et al.*, 2000]. Based on a study of the Holocene sea-level curve and the C^{14} dating of driftwood and mollusc samples of coastal sediments, the long-term (Holocene) uplift rate of the Tainan Tableland is ~5 mm/yr [*Chen and Liu*, 2000]. However, the preliminary result of an InSAR (Interferometric Synthetic Aperture Radar) scan revealed a ground motion of 2.8 cm along the radar line of sight toward the satellite during the period of 1996–1998 [*Fruneau et al.*, 2001]. Under constraints of the measurement of only one campaign mode GPS, they pointed out that the displacement vector of vertical and horizontal components are 32 mm/yr and 16 mm/yr respectively in a period of about two years. Their result indicated an uplift rate of ~16 mm/yr. A dense GPS network survey and precise leveling mode around the Tainan Tableland was established by the Central Geological Survey in Taiwan. The goal of this study is to characterize the deformation pattern and uplift rate of the Tainan Tableland using the InSAR technique within the constraint of the geodetic measurements.

2. Tectonic Setting

[3] The tectonic environment in Taiwan is the result of the collision of the Eurasian Plate (EU) and Philippine Sea Plate (PSP). The PSP moves toward the northwest with respect to the stable EU (Penghu Islands) at the rate of 78.7 mm/yr and the polarity of subduction between the EU and PSP flipped near the central part of Taiwan (Figure 1). The investigated area of SW Taiwan corresponds to the southern part of a Plio-Pleistocene foreland basin which developed in response to lithospheric flexure due to the tectonic loading of the Central Range orogenic belt [*Lin and Watts*, 2002]. The westernmost surface exposures of the fold-and-thrust belt reach the boundary between the Foothills region near the Tainan Tableland [*Sun et al.*, 1998; *Chen and Liu*, 2000]. The Tainan plain can be divided into three major structural grains of different geomorphic features. From the west to the east, there are the Tainan Tableland, the Tawan Lowland and the Chungchou Terrace (Figure 2a). The major part of the Tainan city is on a 30 m high and N-S elongated tableland that is 12.5 km long and 4 km wide with a N20°E trending axis and shows an east-west asymmetry. Its western slope gently dips westward, while the eastern region is obviously steeper and considered as a fault scarp and is mapped as the Houchiali fault [*Chen and Liu*, 2000]. The Tawan Lowland has an average altitude of about 6 m above see-level and the elevation increases eastward and gradually merges with the third unit, the Chungchou Terrace, located between Taiwan Lowland and

[1]Department of Geosciences, National Taiwan University, Taipei, Taiwan.
[2]Department of Civil Engineering, National Chiao Tung University, Hsinchu, Taiwan.
[3]Department of Earth Sciences, National Cheng Kung University, Tainan, Taiwan.
[4]Department of Earth Sciences, University of Oxford, Oxford, UK.
[5]Laboratoire Géomatériaux et Géologie de l'Ingénieur, Universitéde Marne-la-Vallée, Marne-la-Vallée, France.

0094-8276/06/2005GL025613

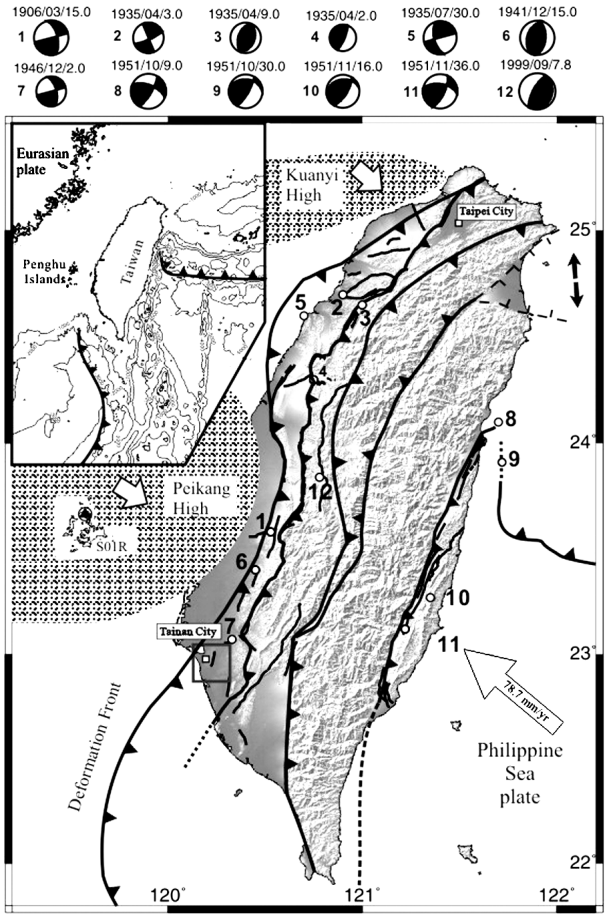

Figure 1. Geodynamic framework and structural map of Taiwan. The rectangle indicates the study area. Open circles, star coded with number indicate destructive earthquakes since 1906. The date (yy/mm) and the focal depth are shown in the upper part of beach ball. Open arrow indicates the rate of the PSP with respect to the S01R of Penghu Islands.

the Western Foothills, the westernmost part of the mountain range of Taiwan (Figure 2a). The Tainan Tableland, Tawan Lowland and Chungchou Terrace are separated by three major thrust faults: the Tainan fault, Houchiali fault, and Chungchou fault [*Chen and Liu*, 2000]. The Tainan fault is considered as the outermost thrust and corresponds to the deformation front of the collision of EU and PSP.

3. Differential SAR Interferometry (D-InSAR)

3.1. Method and Data

[4] For this study, we applied the InSAR technique with a two-pass approach using the programs ROI and SNAPHU [*Chen and Zebker*, 2002]. If there is a spatial displacement on the ground between two acquisitions of SAR images from satellite, we can then measure the displacement by taking the interferometry between two images. By subtracting the topography from the interferogram by using the existing digital elevation model (DEM), thus we can get the displacement along a line of sight (LOS) toward satellite. We call the method the D-InSAR (Differential InSAR) technique [*Massonnet and Feigl*, 1998; *Bürgmann et al.*, 2000]. The satellites ERS-1/2 developed by ESA (European Space Agency) carry the C-band ($\lambda \simeq 5.67$ cm) SAR equipment and can monitor the Earth from an altitude of about 800 km with repeat orbit of 35 days and in nearly all weather conditions.

[5] We use the Taiwan 40 m $\times$ 40 m DEM with a 5 m average height accuracy as the topography in Tainan area which shows the average height of 20 m on the Tainan Tableland. The magnitude of the signal of interferograms is strong and controlled by the baseline of satellites. The shorter baseline distance is more suitable for crustal deformation monitoring, whereas the longer baseline is more suitable for DEM generalization; the shorter baseline pair can result in a better signal [*Zebker et al.*, 1997]. We apply InSAR for crustal deformation, and therefore the short baseline selection is needed. During the interferometry process, the phases due to the topography and the curvature of the earth were removed by the Taiwan 40 m $\times$ 40 m DEM and from the precise orbit from the Delft University, Netherlands.

[6] The InSAR data used in this study consist of six SAR images from a descending orbit (track 232, frame 3145) spanning a time interval of four years (1996–2000), including (A) 16 May 1996; (B) 12 Nov 1998; (C) 21 Jan 1999; (D) 6 May 1999; (E) 28 Oct 1999 and (F) 12 Oct 2000. In order to observe the continuously changing deformation, we choose the image (A) as the master image and other five as slave images in order to obtain the relation of deformation over time in study area. Therefore five interferograms (pairs B-A, C-A, D-A, E-A and F-A) are obtained and correspond to the time span of deformation of 910, 980, 1085, 1260, 1610 days (ambiguity height: 80.1, 103.7, 42.2, 43.2, 103.6 m) from 16 May 1996, respectively. Interferogram patterns are affected by poor image coherence caused by abrupt terrain and dense vegetation in Taiwan. However, several studies have successfully used this technique to demonstrate deformation in an urban area in Taiwan [*Fruneau et al.*, 2001; *Pathier et al.*, 2003]. In the urban area such as the central and northern Tainan Tableland, the phase quality of interferograms is still good enough to detect the crustal deformation in a long time interval (4 years), but in southern Tainan Tableland it is quite poor even for the 2-year pair.

3.2. Coordinate Transformation From LOS into 3-D

[7] The deformation detected by D-InSAR is along the LOS to the satellite, both for descending and ascending orbits, which imply only 1-D information. The advantage of our study is to obtain 3-D deformation in combination with precise GPS horizontal displacement, vertical height changes from leveling and LOS of D-InSAR based on geometric relationship. We derive the equations that can transfer coordinates from LOS into the Cartesian coordinate system. Assume that the displacement vector $\mathbf{V} = (a, b, c)$, so we need to project $\mathbf{V}$ onto the direction of the trace of satellite, denote as (a', b', c'),

$$\begin{aligned} \mathbf{V} &= \begin{bmatrix} a' \\ b' \\ c' \end{bmatrix} = \begin{bmatrix} \cos\phi & \sin\phi & 0 \\ -\sin\phi & \cos\phi & 0 \\ 0 & 0 & 1 \end{bmatrix} \begin{bmatrix} a \\ b \\ c \end{bmatrix} \\ &= \begin{bmatrix} a\cos\phi + b\sin\phi \\ -a\sin\phi + b\cos\phi \\ c \end{bmatrix} \end{aligned} \tag{1}$$

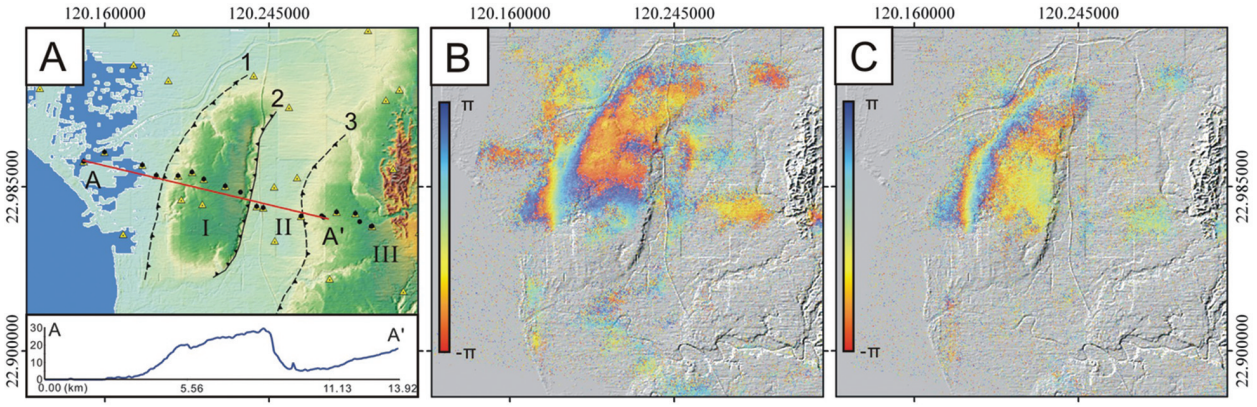

Figure 2. (a) Topographic map and structural units around Tainan area. The yellow triangles represent GPS stations, the black dots represent the leveling benchmarks co-sited with GPS stations. **1**, inferred Tainan fault; **2**, Houchali fault; **3**, inferred Chungchou fault. **I**, Tainan Tableland; **II**, Tawan Lowland, and **III**, Chungchou Terrace. Topographic profile AA′ is shown across the central part of Tainan Tableland. (b) Interferogram B-A (910 days, ha = 80.1 m). (c) Interferogram F-A (1610 days, ha = 103.6 m).

where ϕ is intersection angle between the trace of satellite and the north; a and b are the projection of displacement of GPS along east and north, respectively. a' and b' are the projection of **V** onto parallel and perpendicular the trace of the satellite, respectively. We can now project the displacement onto the LOS,

$$h\cos\theta + (a\cos\phi + b\sin\phi)\sin\theta = \Delta r \tag{2}$$

where Δr is the SRD, which is ideally consistent with the displacement detected by D-InSAR, θ is the viewing angle of satellite, h is the vertical displacement, and we can rewrite (2) as,

$$h = \Delta r\sec\theta - (a\cos\phi + b\sin\phi)\tan\theta \tag{3}$$

from (2) and (3) we can derive the relationship between LOS and Cartesian coordinate system and would imply that we can obtain the vertical displacement from the D-InSAR based on horizontal displacement of the GPS data, even though the GPS data is in sparse distribution relative to the very dense data of D-InSAR in an urban area.

4. Results and Analysis

[8] The five interferograms (B-A, C-A, D-A, E-A and F-A) were obtained and revealed a similarly significant fringe. We selected two D-InSAR pairs (Figures 2b and 2c) from all five interferograms to illustrate the deformation patterns, and can find that the signal is concentrated in an urban area (the northern Tainan Tableland). The southern part and the eastern edge of the Tainan Tableland, the phase coherence is lost. A phase fringe corresponds to a SRD of about 2.8 cm (a phase variation of 2π radians) along the LOS to the satellite. The gradient of the fringe of pair F-A (1610 days) is more remarkable than pair B-A (910 days), which shows continuous uplift and subsidence in study area. For the profile AA′ (Figure 2a), all five interferograms revealed that the SRD trend is uplifted on the Tainan Tableland and relative subsidence on western coastline and Tawan Lowland (Figure 3a) and quite fits the same profile of the topography of the Tainan Tableland (Figure 2a). The exact location of descent is further east from the eastern edge of the Tainan Tableland.

[9] *Rau et al.* [2003] used GPS and precise leveling data to detect the surface deformation and earthquake potential of the Tainan Tableland. On the Tainan Tableland, the GPS data showed the average horizontal velocity is ~12 mm/yr in a direction of 316°. On the eastern edge of Tainan Tableland and toward eastern side, the average horizontal velocity is ~17 mm/yr in a direction of 271° [*Rau et al.*, 2003]. In general, the horizontal velocity on the Tainan Tableland is increasing from west to east at the rate 17~40 mm/yr in a direction of 260°, and the direction of horizontal velocity in the Tainan Tableland is almost perpendicular to the direction of long axis of the Tainan Tableland (N20°E). We adopted GPS horizontal data for the horizontal component constraints to transfer the displacement from LOS into the vertical direction. For ERS-1/2, the

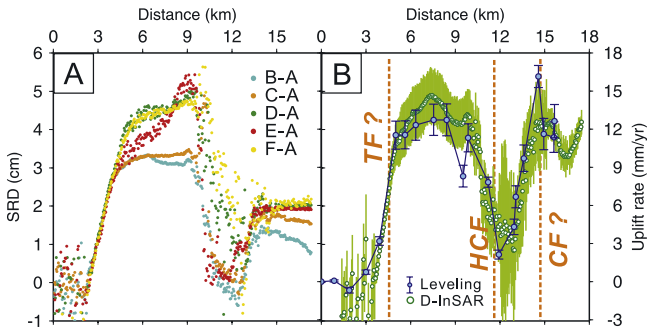

Figure 3. (a) Profile of 5 interferograms after phase unwrapping along AA′ from Figure 2a. (b) Comparison of uplift rate across AA′ between the results of precise leveling data and the vertical displacement from D-InSAR and GPS data. The green belt represents the standard deviation between the 5 profiles, notice the larger standard deviation in the Tawan Lowland, as shown in Figure 2a. TF: Tainan fault(*inferred*); HCF: Houchiali fault; CF: Chungchou fault(*inferred*).

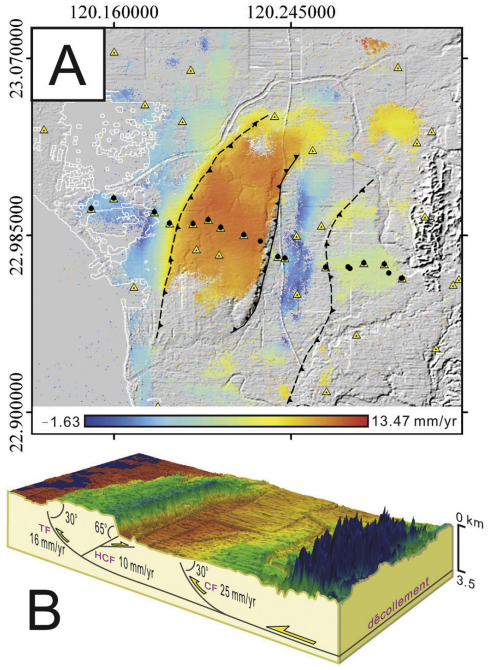

Figure 4. (a) SRD of interferogram after phase unwrapping on shaded topography. (b) An inferred attitudes and slip rates along major faults in a décollement-related pop-up model.

viewing angle (θ) is between 19°∼27° and the direction of descending orbit (ϕ) is N12.5°E, so we substitute these parameters into (3), and we can then obtain the vertical deformation rate along profile AA′. The vertical velocity has a decreasing phenomenon near Houchiali fault and another noticeable diminishing on the east of Houchiali fault (Figure 3a). The velocity also decreased westward on the western edge of the Tainan Tableland and showed a convex shape on the centre of Tainan Tableland with an uplift rate of about 12.48 mm/yr which is slightly larger than the SRD rate. By the precise leveling measurement of 2.41 years (2001–2003) [*Rau et al.*, 2003], the average uplift rate is about 11∼13 mm/yr on the Tableland (Figure 3b). The uplift rate decreased to ∼2.5 mm/yr on the Tawan Lowland. On the Chungchou Terrace, it increased again to 12∼17 mm/yr. The results of precise leveling measurements were quite similar as those from D-InSAR observation in the studied area but slightly smaller on the Tainan Tableland.

5. Discussion and Conclusion

[10] The assessment of seismic hazards of the Tainan Tableland is a crucial topic of concern because of the dense population in Tainan City. The kinematics of structural evolution and the deformation pattern is a fundamental issue to obtain access to this evaluation. Most studies suggested that the diapirism structures occurred onshore and offshore south western Taiwan [*Liu et al.*, 1997; *Chen and Liu*, 2000]. Thus, *Chen and Liu* [2000] suggested that the Tainan Tableland can be interpreted as a mud diapiric dome and the Chungchou Terrace as the product of a blind, thrust fault. They pointed out that from the analysis of radiocarbon ages, the long-term (Holocene) uplift rates of these two terrains are about 5 and 7 mm/yr, respectively, whereas there is a subsidence rate of 1 mm/yr in Tawan Lowland. Based the recent geodetic data [*Fruneau et al.*, 2001; *Rau et al.*, 2003], the short-term uplift rate is obviously larger than the long-term uplift rate deduced from radio carbon dating from the Holocene [*Chen and Liu*, 2000]. In our study, the average uplift rate on central Tainan Tableland is ∼13.5 mm/yr related to the westernmost precise leveling benchmark (Figure 3b). An increasing uplift rate is observed on ∼2 km east of the Houchiali fault from both the leveling data and D-InSAR observation. It is suggested that the branch of the Houchiali fault may develop eastward to Tawan Lowland. The proposed new back-thrust fault should have a shallower dipping angle than that of the Houchiali fault (Figure 4b). Except for the pair D-A and E-A, the SRD shows a linear accumulation trend with time (Figure 3a). In pair E-A the deformation pattern is suddenly increasing on the eastern Tainan Tableland. We consider that this is the result of the remote triggering of the 1999 Chi-Chi Earthquake. (Another pair across the Chi-Chi earthquake showed a similar SRD pattern but is not shown here). However after the earthquake, the deformation became to rebound to the original uplift rate so that we can't find this anomaly in pair F-A.

[11] Our observation of D-InSAR revealed a significant uplift rate of 12∼15 mm/yr on the Tainan Tableland and the uplift rate of ∼2 mm/yr on the Tawan Lowland (Figure 4a). The gradient of the deformation across the edge of the Tainan Tableland increase dramatically (Figure 2a), thus a décollement-related ramp and a pop-up model is proposed (Figure 4b). This pop-up structure is also suggested by the data of seismic reflections, surface geology and subsurface well [*Huang et al.*, 2005]. We conclude that the on-land anticlines and the offshore elongated ridges have an identical tectonic origin with initiation along NE trending folds and thrusts resulted from the movement of the major décollement, which is generated by the collision of two plates.

[12] Based on the 2-D analytical solution [*Cohen*, 1996] and the inferred fault geometry, the slip rate along the inferred TF is 16 mm/yr, 10 mm/yr along HCF, and 25 mm/yr along the inferred CCF (Figure 4b). Thus we propose that growing of the Tainan Tableland is mostly resulted from the freely slipping of the TF and the HCF. The locking depth should be located on the deeper part of décollement, eastern of the CCF. In addition, the combination of D-InSAR, GPS data and the precise leveling data reveals that the short-term deformation rate is larger than long-term deformation rate, which implies that a destructive seismic event could occur in the eastern Tainan area. Further work will concentrate on more complete SAR image analysis and the dense GPS survey.

[13] **Acknowledgments.** We are grateful to Editor Eric Calais and an anonymous reviewer for constructive comments that help significantly improve our manuscript. We also thank to Jacques Angelier, Yu-Chang Chan, and Chung-Pai Chang for their suggestions and discussions. This research was supported by grants from the National Science Council of Taiwan (NSC 91-2119-M-002-020) and the Central Geological Survey of the MOEA.

References

Bürgmann, R., P. A. Rosen, and E. J. Fielding (2000), Synthetic aperture radar interferometry to measure Earth's surface topography and its deformation, *Annu. Rev. Earth Planet. Sci.*, *28*, 169–209.

Chen, C.-W., and H. A. Zebker (2002), Phase unwrapping for large SAR interferograms: Statistical segmentation and generalized network models, *IEEE Trans. Geosci. Remote Sens.*, *40*, 1709–1719.

Chen, Y.-G., and T.-K. Liu (2000), Holocene uplift and subsidence along an active tectonic margin southwestern Taiwan, *Quat. Sci. Rev.*, *19*, 923–930.

Cohen, S. C. (1996), Convenient formulas for determining dip-slip fault parameters from geophysical observables, *Bull. Seismol. Soc. Am.*, *86*, 1642–1644.

Fruneau, B., E. Pathier, D. Raymond, B. Deffontaines, C.-T. Lee, H.-T. Wang, J. Angelier, J. P. Rudant, and C.-P. Chang (2001), Uplift of Tainan Tableland (SW Taiwan) revealed by SAR interferometry, *Geophys. Res. Lett.*, *28*, 3071–3074.

Huang, S.-T., K.-M. Yang, J.-H. Hung, J.-C. Wu, H.-H. Ting, W.-W. Mei, S.-H. Hsu, and M. Lee (2005), Deformation front development at the northeast margin of the Tainan basin, Tainan-Kaohsiung area, *Taiwan Mar. Geophys. Res.*, *25*, 139–156, doi:10.1007/s11001-005-0739-z.

Lin, A.-T., and A. B. Watts (2002), Origin of the west Taiwan basin by orogenic loading and flexure of a rifted continental margin, *J. Geophys. Res.*, *107*(B9), 2185, doi:10.1029/2001JB000669.

Lin, C.-W., H.-C. Chang, S.-T. Lu, T.-S. Shih, and W.-J. Huang (2000), An introduction of the active faults of Taiwan, *Spec. Publ. Cent. Geol. Surv.*, *13*, 122 pp.

Liu, C.-S., I. L. Huang, and L. S. Teng (1997), Structureal features off southwestern Taiwan, *Mar. Geol.*, *137*, 305–309.

Massonnet, D., and K. Feigl (1998), Radar interferometry and its application to changes in the Earth's surface, *Rev. Geophys.*, *36*(4), 441–500.

Pathier, E., B. Fruneau, B. Deffontaines, J. Angelier, C.-P. Chang, S.-B. Yu, and C.-T. Lee (2003), Coseismic displacements of the footwall of the Chelungpu fault caused by the 1999, Taiwan, Chi-Chi earthquake from INSAR and GPS data, *Earth Planet. Sci. Lett.*, *212*, 73–88.

Rau, R.-J., K.-E. Ching, T.-H. Hsieh, C.-I. Yu, C.-S. Hou, Y.-H. Lee, J.-C. Hu, Y.-C. Chan, J.-C. Lee, and J.-H. Hung (2003), Surface deformation and earthquake potential of Tainan Tableland, southwestern Taiwan, *Spec. Publ. Cent. Geol. Surv.*, *14*, 161–171.

Sun, R., Q.-C. Sung, and T.-K. Liu (1998), Near-surface evidence of recent Taiwan Orogeny detected by a shallow seismic method, *Earth Planet. Sci. Lett.*, *163*, 291–300.

Zebker, H. A., P. A. Rosen, and S. Hensley (1997), Atmospheric effects in interferometric synthetic aperture radar surface deformation and topographic maps, *J. Geophys. Res.*, *102*, 7547–7563.

B. Deffontaines, and B. Fruneau, Laboratoire Géomatériaux et Géologie de l'Ingénieur, Université de Marne-la-Vallée, F-77454 Marne-la-Vallée, France.

K.-E. Ching and R.-J. Rau, Department of Earth Sciences, National Cheng Kung University, Tainan 701, Taiwan.

C.-S. Hsieh, Department of Civil Engineering, National Chiao Tung University, Hsinchu 300, Taiwan.

M.-H. Huang and J.-C. Hu, Department of Geosciences, National Taiwan University, Taipei 106, Taiwan. (r93224213@ntu.edu.com)

E. Pathier, Department of Earth Sciences, University of Oxford, Parks Road, Oxford OX1 3PR, UK.